Single-cell Profiling Reveal Types of Interstitial Cells in Human and Rat Bladder

Zhenxing Yang
Army Medical University
Ye Gao
Army Medical University
Peilin Liu
Army Medical University
Weisheng Jia
Army Medical University
Zhenqiang Fang
Army Medical University
Jiang Zhao
Army Medical University
Jiangfan Zhong
University of Southern California
Yuanyuan Zhang
Wake Forest School of Medicine: Wake Forest University School of Medicine
Longkun Li (lilongk@tmmu.edu.cn)
Army Medical University

Research article

Keywords: Single-cell RNA-seq, Bladder, Interstitial cells

Posted Date: September 22nd, 2020

DOI: https://doi.org/10.21203/rs.3.rs-74172/v1

Abstract

Backgrounds:

The mechanism underlying bladder urination pathophysiologies has not been understood yet because the types of interstitial cells present in the bladder are still obscure.

Results:

Here, we classified the cell types in the bladder without bias using 10x genomics single-cell RNA-seq and identified 35,510 and 19,946 cells from human and rat bladder tissues, respectively. In addition to the major cell clusters including urothelial cells, smooth muscle cells, endothelial cells, neurons, and immune cells, three types of interstitial cells were identified in this study. Fibroblasts and myofibroblasts were shown to occupy large proportions of interstitial cells, located mainly between the epithelial strata and muscle strata. A new type of interstitial cell, Mki67^{+}, which was found both in human and rat bladder tissues, may participate in bladder disease development.

Conclusions:

Our investigation thus lays the ground work for identifying the cell types in bladder tissues and provides potential clues to understand abnormal bladder functions.

Background

Filling and voiding of urine in the bladder depends on the coordinated activity of complex neural control systems in the spinal cord and peripheral neurons, as well as muscle cells and epithelial stratum cells [1]. Smooth muscle cells are necessary for bladder function and increased excitation-contraction coupling in the detrusor muscle leads to voiding of urine from the bladder. Moreover, the epithelial stratum represents a blood–urine barrier preventing reabsorption of noxious compounds from the urine and also plays a role in sensory function. This function is implemented by the expression of numerous receptors/ion channels that act as neuronal sensor molecules [2]. In contrast, the function of interstitial cells in the bladder is controversial [3]. Research is definitely required to fully understand the location, molecular markers, functions, and role of interstitial cells, as well as their contribution to spontaneous contractions of the bladder. Previous studies have introduced inconsistencies in the terminology of interstitial cells such as interstitial cells (ICs), interstitial cells of cajal (ICC)-like cells, interstitial cells of cajal (ICCs), myofibroblasts, pacemaking cells, telocytes (TCs), fibroblast-like cells (FLC), and myoid cells [4–9]. So far, no clear bladder cell classification has been established considering the types of interstitial cells.

Molecular markers such as c-Kit, *PDGFRα*, Desmin, Vimentin, cGMP, and *CD34* have been used to label interstitial cells, but their results have been inconsistent [7]. Traditional research methods including immunohistochemistry (IHC), immunofluorescence (IF), transmission electron microscopy (TEM), and patch clamp technology are insufficient to determine the bladder cell types. With the development of

single-cell RNA-seq (scRNA-seq) technology, the 10x Genomics platform allows unbiased classification of cell types from clusters of single cell suspensions. Subsequently, with the assistance of next-generation sequencing (NGS), a massive amount of RNA-seq data can be easily handled and analyzed for visualization. Therefore, this study aimed to explore the cell types in bladder tissues that can provide new insights into bladder organization and disease occurrences.

Results

Identification of cell types in human and rat bladders

After strict filtering and quality control, a total of 35,510 cells from two human (one male and one female) and 19,946 cells from two rat (one male and one female) bladder tissues were obtained for further clustering (Fig. 1, Fig. S1 and Supplementary Table 1). The cells were separated from zones of the bladder anterior wall in the human bladder and from the overall bladder in rats, and was then digested to a single cell suspension, which was subjected to scRNA-seq on the 10x Genomics platform version 3.0 (Fig. 1a). On average, we detected 2,340 genes from human and 1,996 genes from rat single cells (Supplementary Table 1). Subsequently, unsupervised clustering analysis showed 26 and 23 clusters in all filtered human and rat cells, separately (Fig. S1a and Fig. S1f). Cells from different sexes were distributed evenly in the same cluster and showed minimal differences (Fig. S1b and Fig. S1g). According to the characterization of the bladder histological structure and marker genes from reference (Supplementary Table 2), we identified 13 major cell clusters in human and 14 major cell clusters in rat (Fig. 1b-1e). The number and type of cells show minimal differences between human and rat (Fig. 1f, Fig. S1d-S1e, Fig. S1i-S1j).

To further analyze the features of major cell clusters from human and rat bladders, we performed pseudotime trajectory, CD markers, cell junctions, ion channels, cell surface receptors, and transcription factor distribution among different clusters. To clarify the states and relationships between the major cell clusters in humans and rats, 3 major states were identified using pseudotime trajectory (Fig. 2a-2b, Fig. S2a and S3a), indicating the cells undergoing different developmental and differentiation stages. Pearson correlation analysis showed high consistency between homologous cell types of human and rat bladder tissues (Fig. 2c). In addition, CD molecular markers can specifically label cell populations in human or rat bladder tissues, such as *CD24*, *CD138,* and *CD358* for epithelium stratum cells; *CD364* and *CD91* for fibroblasts; *CD362* and *CD121a* for myofibroblasts; and *CD146* for smooth muscle cells (Fig. 2d and 2g). The intercellular junction complex between bladder cells plays a key role in adhesion and barrier function and consists of adherent junctions, gap junctions, desmosomes, and tight junctions. We found that homologous genes of *CLDN4*, *CLDN7*, *F11R*, *GJB2*, *GJB6*, and *OCLN* were expressed in epithelial stratum cells; *GJC1*, *GJA4*, and *JAM3* were expressed in smooth muscle cells; *PANX1* was expressed in fibroblasts, and *JAM2* was expressed in endothelial cells of both humans and rats (Fig. 2e and 2h). One of the main functions of epithelial and smooth muscle cells in the bladder is ion transport and sensory transduction. We also identified the water transporter *AQP3*, epithelial sodium channel *SCNN1A*, potassium two pore domain channel *KCNK1*, chloride voltage-gated channel *CLCN3* expressed in

epithelial stratum cells, *CACNA1H*, *P2RX1*, *KCNJ8*, and *ITPR1* expressed in smooth muscle cells, *TRPA1* expressed in myofibroblasts, *PKD2* expressed in fibroblasts, *AQP1*, and *ORAI3* expressed in endothelial cells (Fig. 2f and 2i). Regarding transcription factors, the expression profile among the major cell clusters in humans and rats were revealed to be similar to each other (Fig. 2j and 2n). Comparison of expression profiles between different genders in human and rat samples showed that the Pearson coefficient was 0.98 (Fig. 2K, $P < 0.001$) in human and 0.98 (Fig. 2O, $P < 0.001$) in rat. Gene Ontology (GO) enrichment analysis indicated that genes with higher expression in the human male bladder were associated with muscle contraction (Fig. 2l), genes with higher expression in the human female bladder were associated with extracellular structure organization (Fig. 2m), genes with higher expression in the rat male bladder were associated with wound healing (Fig. 2p), and genes with higher expression in the rat female bladder were associated with metabolic processes (Fig. 2q).

Characterization of epithelial stratum cells in the human and rat bladder

To identify the subpopulations of epithelial stratum cells in human and rat, second-level clustering was performed, which distinguished the epithelial stratum cells into three clusters including umbrella, intermediate, and basal cells (Fig. 3a and 3b, Fig. S4). Umbrella cells in human (n = 1139) and rat (n = 3380) bladder highly express uroplakin proteins (*UPK1A*, *UPK1B,* and *UPK2*), which cover the apical plasma membrane and reducing membrane permeability (Fig. 3c and 3e). GO pathway enrichment indicated that the functions of signal transduction and protein secretion were enriched in umbrella cells (Fig. 3g and 3i). Basal cells in human (n = 686) and rat (n = 5075) bladder tissues highly expressed the protein members of the keratin gene family (*KRT5* and *KRT17*), which are widely distributed during the differentiation of simple and stratified epithelial tissues (Fig. S4). GO pathway enrichment indicated that the basal cells interacted with neurons, responding to ion and hormone signaling (Fig. 3h and 3k). Pseudotime trajectory analysis demonstrated that umbrella and basal cells appeared at the end of the branch and intermediate cells at the continuations (Fig. 3d and 3f), which may indicate development and differentiation direction among the three types of cells. However, this assumption needs further validation. There is no clear boundary regarding CD markers, ion channels and receptors, cell junctions, and transcription factors among the three types of epithelial stratum cells (Fig. S16f- S16l).

Characterization of fibroblasts in human and rat bladder

The marker genes for distinguishing fibroblasts are *SFRP2*, *MMP2*, *COL1A*, and *PDGFRA* (Fig. S5a-S5b). In addition, algorithmically identified marker genes for bladder fibroblast include *GSN*, *DCN*, *PI16* (*CD364*), and *LRP1* (*CD91*) (Fig. S5c-S5d) in both human or rat bladder tissues. Second-level clustering showed 5 subpopulations of fibroblasts in human and 4 in rat (Fig. 4a and 4b). The marker gene expression levels among subpopulations of fibroblast showed ambiguous boundaries, but high expression level of *A2M* gene in fibroblast_3 of human and fibroblast_1 of rat and high expression level of *FOS* gene in

fibroblast_2 of human and fibroblast_3 of rat (Fig. 4c and 4e) were observed simultaneously. We did not find any significant difference of states in the subpopulations of fibroblasts in the following pseudotime trajectory analysis (Fig. 4d and 4f). Interestingly, GO enrichment analysis of special marker genes in the subgroups of fibroblasts showed cell response stimuli for hormones (Fig. S14a), chemokines (Fig. S14b, S14e), calcium ions (Fig. S14a, S14g), leukocytes (Fig. S14c, S14f), zinc ions (Fig. S14c), *TGFβ* (Fig. S14d, S14h), and so on. It thus seems like fibroblasts can respond to different stimuli, but their role in bladder signaling transduction still needs further clarity. We did not find any special CD markers, ion channels and receptors, cell junctions, and transcript factors to distinguish the subpopulations of fibroblasts in human and rat samples (Fig. S14i- S14n).

Fibroblasts are one of the main interstitial cells in the bladder. Therefore, it is important to determine their location in bladder tissue. Double immunofluorescence staining performed with anti-*THY1* (only expressed in fibroblast) and anti-*DES* (only expressed in smooth muscle cells) antibody in human bladder tissue indicated that fibroblasts are located under the epithelial stratum and among muscular bundle cells (Fig. 4g). Immunohistochemical staining performed with anti-*THY1* antibody confirmed this finding (Fig. 4h). Flow cytometric sorting of cells from a single cell suspension of human bladder cells using anti-*THY1* (CD90) antibody showed a fibroblast-like cell type presentation as a sheet-like body with prominent cytoplasm, abundance of mitochondria and prominent rough and smooth endoplasmic reticulum (Fig. 4i). Similarly, rat bladder tissues stained with double immunofluorescence (anti-LBP and anti-*Des*) indicated the same location as that determined in human bladder tissues (Fig. 4j).

Characterization of smooth muscle cells in human and rat bladder

Marker gene (*DES*, *MYH11*, *MYL9*, *TAGLN*, *TPM2*, *ACTA2*, *ACTG2,* and *CNN1*) expression levels showed consistency in human and rat smooth muscle cells (SMCs) (Fig. S6). Five subpopulations of SMCs were present after second-level clustering in both human and rat SMCs (Fig. 5a and 5b). SMCs in the bladder may exist in the artery, vein, lymphatic vessels, detrusor muscle, and even in the muscularis mucosae located in the lamina propria. All sub-clusters of SMCs appeared at the end of the branch in the state of pseudotime trajectory analysis (Fig. 5d and 5f), indicating that they are mature terminally differentiated cells. However, these cannot be distinguished based only on algorithmically identified marker genes (Fig. 5c and 5e). GO enrichment pathway analysis may provide some clues (Fig. 15s). SMC_1 in human tissues shows higher Pearson correlation coefficients with SMC_1 in rat (Fig. S3d), cells in this cluster are associated with artery/vein vascular development and also on zinc ion response (Fig. S15a and S15f). SMC_2 in human tissues correlated with SMC_2 in rat tissues (Fig. S3d), cells in SMC_2 are associated with muscle contraction and striated muscle tissue development (Fig. S15b and S15g). SMC_3 in human is related with SMC_3 in rat (Fig. S3d) and cells in SMC_3 are associated with leukocyte chemotaxis and vascular development (Fig. S15c and S15h), which indicated that the sources of SMC_3 may originate from lymphatic vessels. SMC_4 in human parallels with SMC_4 in rat (Fig. S3d); cells in SMC_4 are associated with response to type I interferon and endopeptidase activity (Fig. S15d and S15i). SMC_5 in

human and rat function with extracellular structure organization, cell-substrate adhesion, and so on (Fig. S15e and S15j). It most likely that SMC_5 are the kind of cells located in the muscularis mucosae, which participate in wound healing and tissue repair. CD markers, ion channels and receptors, cell junctions, and transcription factor classification analysis showed that SMC_5 was significantly different from other clusters (Fig. S15k-o). Therefore, functions of this cluster in the bladder need further investigation.

Characterization of endothelial cells in human and rat bladder

Common marker genes (*SELE*, *VCAM1*, *CDH5,* and *ENG*) are expressed in endothelial cells consistently within human and rat bladder tissues (Fig. S8a and S8b). Algorithmically identified marker genes in human (*ACKR1*, *TM4SF1*, *IFI27* and *STC1*) and rat (*Tm4sf1*, *Plvap*, *Selp* and *Cst3*) show differences between each other. Three subpopulations of endothelial cells were present after second-level clustering in both human and rat (Fig. 6a and 6b), which may correspond with the artery, vein, and lymphatic vessels. The difference among these three subpopulations of endothelial cells is obscure (Fig. 6c and 6e). However, pseudotime trajectory analysis (Fig. 6d and 6f) indicated that they are mature terminally differentiated cells distributed at the end of the branch, respectively. Interestingly, GO analysis indicated that endothelial cells_1 in human and rat are majorly associated with leukocyte migration and response to lipopolysaccharide, which demonstrates that these clusters may include a kind of endothelial cell in lymphatic vessels (Fig. 6g and 6j). Endothelial cells_2 in human and endothelial cells_3 in rat showed high correlation (Fig. S3d) and GO analysis showed that these clusters were associated with notch signaling pathway and angiogenesis (Fig. 6h and 6l). Endothelial cells_3 in human and endothelial cells_2 in rat were correlated with each other (Fig. S3d) and GO analysis showed these clusters were associated with wound healing and extracellular structure organization (Fig. 6i and 6k). CD markers, ion channels and receptors, cell junctions, and transcription factor classification analysis showed that endothelial cells_3 in human and endothelial cells_2 in rat showed a significant difference compared with other clusters (Fig. S16a-S16e), indicating that these clusters may be a kind of endothelial cells in the artery.

Characterization of myofibroblasts in human and rat bladder

There is an ongoing debate about the occurrence of true myofibroblasts in the bladder. The key feature of these essentially reactive cells is the fibronexus. Myofibroblasts express marker genes (*ACTA2*, *ACTG2*, *TAGLN* and *PDGFRB*) that exist in both muscle cells and fibroblasts (Fig. S7A-S7B). Algorithmically identified marker genes in human (*STC1*, *AREG*, *PLAT* and *TBX3*) and rat (*Cxcl14*, *Tgfbi*, *Crayb* and *Car3*) showed a special relation between each other (Fig. 7d, 7e, Fig. S7c-S7d). The gene expression Pearson coefficient between human and rat myofibroblasts was 0.77 (Fig. 7A, $P < 0.001$), which denotes the difference in the two kinds of myofibroblasts. However, GO analysis of marker genes in human (Fig. 7b) and rat (Fig. 7c) myofibroblasts demonstrated simultaneous enrichment in the extracellular matrix

organization, which suggests that they have the same function in the bladder. To locate myofibroblasts in the bladder, antibodies against TRPA1 (specifically expressed in human myofibroblast), DES, and Tgfbi were used for double immunofluorescence staining. The results showed that myofibroblasts were located mainly between the epithelial stratum and muscle stratum. However, the function of myofibroblasts in the process of bladder contraction needs further validation. Myofibroblasts showed similar features between human and rat, i.e. common CD markers (*CD362* and *CD121a*) as mentioned before (Fig. 2d and 2g), common junction proteins of *GJC1*, J*AM3,* and *CLDN11* (Fig. 2e and 2h). However, considering the receptor and ion channel, the expression level of *TRPA1* and *KCNF1* was higher in the human myofibroblast; in contrast, the expression level of *Grin2c*, *Kcnq5,* and *Kcnma1* was enriched in rat myofibroblasts (Fig. 2f and 2i).

Characterization of Mki67$^+$ cells in human and rat bladder

Surprisingly, a new cell type, Mki67$^+$ cells, were found both in the human and rat bladder tissues (Fig.1b and 1d). These cells demonstrated a clear boundary distinguished from other clusters and also showed a reliable mean UMI value (Fig. S1a, S1c, S1f and S1h). The Pearson correlation of gene expression for Mki67$^+$ cells between human and rat was 0.74 (Fig. 8a). However, GO analysis of marker genes demonstrated enrichment mainly in the pathway of chromosome segregation and cell division in human and rat, separately (Fig. 8b and 8c) which coincides with the feature of Ki-67 protein, which is widely used as a proliferation marker. Algorithmically identified marker genes in human (*MKI67* and *BIRC5*) and rat (*Mki67* and *Clca5*) tissues shows a difference between each other (Fig. 8d and 8e). We also performed immunofluorescence and immunohistochemical staining with anti-MKI67 antibody to locate the position of Mki67$^+$ cells in bladder tissues. The results showed that Mki67$^+$ cells lie in the mucosal layer and also within the muscle bundle (Fig. 8f and 8g). Despite this long-standing characterization of Ki-67 protein, to our knowledge, this is the first report showing that Mki67$^+$ cells exist in the bladder, and these should be investigated for their cellular functions.

Characterization of other types of cells in human and rat bladder

In addition to well-known cells in bladder tissues, we also found neurons and clusters of immune cells such as T cells, B cells, monocytes, mast cells, macrophages, and granulocytess (Fig.1b and 1d). The marker genes used to distinguish neurons are *GPM6A* and *RELN*, and the algorithmically identified marker genes are *CCL21*, *MMRN1*, *CLDN5*, and *LYVE1* which coincide with each other in human and rat (Fig. S9a-S9d). The Pearson correlation coefficient between human and rat neuron is 0.77 (Fig. S9e), and GO analysis shows that these neuronal cells are mainly focus on the regulation epithelial cell proliferation, ion homeostasis, vascular and muscle development (Fig. S9f and S9g). The B cells marker genes include *CD79A*, *MZB1*, *MS4A1,* and *CD19* (Fig. S10a), and the algorithmically identified marker genes are *IGLC2*, *IGKC*, *IGLC3,* and *IGHA1* (Fig. S10b). T cell marker genes include *CD3D*, *CD3E*, *CD3Gm*

and *CD8A* both in human and rat (Fig. S12a and S12b). Three genes (*CD14*, *CD163,* and *MS4A7*) were selected as markers of monocytes both in human and rat (Fig. S13a and S13b). Two genes (*Cd68* and *Cd74*) from reference (Fig. S13c) and two specific marker genes (*RT1-Da* and *RT1-Db1*) were selected to mark rat macrophages (Fig. S13d). Four specific marker genes (*S100A9*, *G0S2*, *SRGN* and *S100A8*) were selected as markers for human granulocytes (Fig. S13e). Four genes (*Mt-atp6*, *Mt-co1*, *Mt-co2*, and *Mt-co3*) were selected to mark rat adipose tissue cells (Fig. S13f).

The special marker gene KIT must be given more attention because c-kit$^+$ interstitial cells of cajal are reported distributed in the bladder interstitial region. We luckily found a cluster of c-kit$^+$ cells (Fig. S11a) in the human sample. However, further bioinformatics analysis showed that these clusters of cells express marker genes (*ENPP3*, *FCER1A* and *SLC18A2*) similar to the markers of mast cells (Fig. S11a). GO and KEGG pathway analysis suggested that these are cells associated with mast cell migration, activity, and mast cell mediated immunity (Fig. S11c and S11d). So, we considered these clusters of cells as mast cells.

Discussion

In the current study, scRNA-seq technology was employed to map the transcriptional landscape of human and rat bladder cells. In all, 35510 cells from human and 19946 cells from rat bladder tissues were captured and filtered for subsequent clustering, and 13 and 14 major cell clusters were identified in human and rat, respectively. In addition to the commonly reported cell types (umbrella cell, intermediate cell, basal cell, smooth muscle cell, endothelium cell and immune cells), we found interstitial cells including fibroblasts, myofibroblasts, and newly discovered the mki67$^+$ cells.

Although the cell types clustered in human and rat tissues did not show one to one correspondence, the major cell clusters were coincident with each other. Unsurprisingly, three clusters of the epithelial stratum cells were identified in bladder tissues, which were coincident with histological observation. Umbrella cells showed several key features in maintaining normal barrier function as bladder filling and emptying. We found special marker genes expressed only in the epithelial stratum, which included a number of uroplakin proteins (*UPK1A*, *UPK1*, and *UPK2*), junction proteins (*CLDN4*, *CLDN7*, *F11R*, *GJB2*, *GJB6*, and *OCLN*), and CD molecular markers (*CD138* and *CD358*) for cell sorting regardless of human or rat origin. Simultaneously, the water transporter *AQP3*, epithelial sodium channel *SCNN1A*, potassium two pore domain channel *KCNK1*, and chloride voltage-gated channel *CLCN3* were identified in the epithelial stratum cells, which provides basic information for further evaluation. Previous researchers have suggested that basal cells remain in the basement membrane and play the role of undifferentiated cells, which can replenish the lost surface cells. However, a recent fate mapping study demonstrated that an intermediate type of cells, which are also relatively undifferentiated, contain the progenitor population for replacing umbrella cells [10]. Interestingly, pseudotime trajectory analysis of epithelial stratum cells in the current investigation suggests that intermediate cells can differentiate into umbrella or basal cells.

Alternatively, the population of interstitial cells in the bladder is increasingly interesting because these cells have been proposed to participate in the spontaneous contraction activity of the bladder [7]. Interstitial cells have been proved to exist in the bladder of human and guinea pig [11–13]. Along with immune-related cells, three types of suburothelial interstitial cells including fibroblasts, myofibroblasts, and Mki67$^+$ cells were identified. Buoro et al. first reported the existence of myofibroblasts in the bladder in 1993 [14] and these cells stain for vimentin and α-smooth muscle actin, but not for desmin [15]. More importantly, the scRNA-seq data show that myofibroblasts express the special CD markers *CD362* and *CD121a*, the special junction proteins *JAM3*, *GJC1*, and *PANX1*, and the special receptor *TRPA1*. Connexin 43 proteins (*GJA1*), Cadherin-11(*CDH11*), P2Y6 receptors, and M3 muscarinic receptors (*CHRM3*) were absent or low expressed in the current research [16, 17]. In summary, myofibroblasts in the submucosal layer of the bladder are linked by gap junctions consisting of JAM3, *GJC1*, and *PANX1* with muscle cells and fibroblasts, suggesting a network of functional connection among these cells, immediately below the urothelium. Drake et al. have reported the morphology, phenotype and ultrastructure of fibroblasts in the human bladder, which was coincident with the current findings [18]. We found that fibroblasts have the special markers *PDGFRα*$^+$/*COL1A2*$^+$/*MMP2*$^+$/*SFRP2*$^+$, the CD markers *CD364*, *CD91*, and *CD90*, and the cation channel *PKD2*. *CD90*$^+$ fibroblasts were cultured and ultrastructurally showed a sheet-like body with prominent cytoplasm, abundance of mitochondria, and prominent rough and smooth endoplasmic reticulum with a moderately electron dense amorphous content and prominent Golgi complexes. Regarding their location, fibroblastic cells were observed within the lamina propria and throughout the smooth muscle and connective tissue. No specific junction with nerve fibers or smooth muscles was found in fibroblasts. Pathway analysis indicated that fibroblastic cells that respond to different signaling stimuli can interact with smooth muscle cells, epithelium cells, and neurons, but the role of fibroblasts in the bladder still needs further validation. Fibroblasts and myofibroblast are also found in the detrusor layer. Cells expressing the marker c-Kit were proved as mast cells. Although we did not find c-Kit$^+$ interstitial cells in the current research, we cannot ensure that such cells do not exist in the bladder because of the potential technological limitations discussed below. However, the recent 3D-electron microscopic characterization of interstitial cells does not support the incidence of ICC-like cells in the upper lamina propria of the human bladder [19]. Thus, whether c-Kit$^+$ interstitial cells exist in the detrusor layer still needs further investigation.

A new type of interstitial cells, Mki67$^+$ cells were found in the current clustering in both human (n = 32) and rat (n = 140) samples. Similar to fibroblasts and myofibroblasts, Mki67$^+$ cells were located in the submucosal layer and throughout the smooth muscle and connective tissue of the bladder. Ki-67 is identified as a proliferation marker that is highly expressed in cycling cells but is strongly downregulated in resting G0 cells [20]. The multiple molecular functions of Ki-67 display cell type-specific variations and are correlated with distinct stages of the cell cycle, which is coincident with the current pathway analysis. Our discovery first indicated that Ki-67 protein represents a new cluster of cells that may provide more information about their function. Recent research has shown that *MKI67* mRNA is a promising prognostic marker in bladder superficial urothelial cell carcinoma, because increased MKI67 mRNA concentrations

indicate short recurrence-free periods. Whether the conclusion mentioned above indicates that *Mki67*$^{+}$ cells proliferate in urothelial cell carcinoma of the bladder still needs validation.

The current study has some limitations. First, some types of cell were captured disproportionately between human and rat tissues, such as the epithelial stratum cells, fibroblasts, and smooth muscle cells. This is mainly because of the difficult process of tissue digestion. A large amount of connective tissues are present in the bladder, so it is likely that biases are introduced by the different tissue dissociation protocols used [21, 22]. We used a combination of enzymatic dissociation that can avoid biases of the cell populations captured for scRNA-sEq. However, bladder detrusor cells within a bundle are connected together to form a functional syncytium, which determined the difficulty of digestion. Only a little part of smooth muscle cells was attributed to the detrusor, because a large ratio of captured muscle cells may come from vascular, and even from the muscularis mucosae where smooth muscle fascicles exist freely [23]. Second, only the bladder anterior wall tissues were captured and digested for analysis because of the cost and sample source; thus, we could not ensure that all cell types were present in the human bladder tissues obtained. Further, the structure from the bladder neck and urethral sphincter differs from that at the anterior wall, which may lead to the absence of some important cell types related to urination control. However, the whole bladder from rats was analyzed for clustering, and we did not find any significant difference between the rat and human samples.

Conclusions

In conclusion, identifying cell types of bladder is helpful for understanding the pathophysiology. In current paper, we not only answered questions regarding the types of bladder interstitial cells, but also discovered new types of Mki67^{+} cells. Future studies may focus on the function of each type of cells and the mechanism of taking part in the pathological changes.

Methods

Samples

Two normal bladder anterior wall tissues (one male and one female) were donated by two patients who underwent open radical cystectomy. The current investigation was conducted with the approval of the medical ethics committee of the Second Affiliated Hospital of the Army Medical University. Each patient signed a written informed consent form before donating their tissues for this study. For detailed information about the patients, see supplementary information.

Two Sprague Dawley rats (6 months old, one male and one female) were purchased from the Laboratory Animal Center of the Third Afflicted Hospital at the Army Medical University. Rats were group-housed under a 12-h light/dark cycle and provided with water and food. All experimental procedures were approved by the Army Medical University Animal Care and Use Committee and were performed in accordance with the Institutional Animal Welfare Guidelines.

Tissue preparing, handling, and enzymatic isolation

Rats were sacrificed by cervical dislocation. The bladder tissues were isolated from the sacrificed rats under aseptic conditions and placed in sterile PBS (phosphate buffered saline) (Gibco, pH 7.4 basic, #lot8119170, China). Using sterile forceps and either small sterile scissors or a sterile scalpel, the bladder tissue was minced to small pieces. The minced bladder tissue was transferred to a 50 ml tube for the following enzymatic digestion.

Donor bladder tissues from humans (size 1 cm x 1 cm x 1 cm) were collected in DMEM-high glucose medium (Gibico, #lot8119079, China) containing 10% FBS (Gibico, #lot2017490C, Australia) and 5 μg/ml gentamicin (Gibco, #lot2023926, USA). The wells of a sterile 6-well plate were pre-filled with 10 ml of pre-warmed tissue washing medium (PBS and 5 μg/ml gentamicin). The tissue was gently agitated in the well using a sterile forceps for 5–10 s; successive washing of the tissue was continued through each unused well until all six wells were used. Using a sterile forceps and either small sterile scissors or a sterile scalpel, the bladder tissue was minced into small pieces. Minced bladder tissue was transferred to a 50 ml tube for following enzymatic digestion.

Tissues from rats and human were digested for about 4 hours at 37°C with agitation in a digestion solution containing 2 mg/ml papain (Worthington, #lotLS003120), 100 U/ml Collagenase II (Sigma, CAS No: 9001-12-1, USA), and 100 U/ml Collagenase IV (Sigma, CAS No: 9001-12-1, USA) in DMEM-high glucose medium [24]. The digested suspension was passed through a 60 μm Steriflip (Millipore, CAS No: SCNY00060), washed twice with washing medium (PBS and 0.04% BSA). Enriched live cells were washed and counted using a hemocytometer with trypan blue. Overall, it took 6-7 hours from obtaining the tissues to generating single cell suspensions run on the Chromium 10X device.

Library preparation and sequencing

After digesting, the single cell suspension was used for the quality check and counting; the cell survival rate was generally above 80%. Cells were loaded onto the 10X Chromium Single Cell Platform (10X Genomics, https://www.10xgenomics.com /resources/ support-documentation/) at a concentration of 1,000 cells/μl (Single Cell 3' library and Gel Bead Kit v.3) followed by the manufacturer's protocol. Generation of gel beads in emulsion (GEMs), barcoding, GEM-RT clean-up, complementary DNA amplification, and library construction were all performed according to the manufacturer's protocol. Qubit was used for library quantification before pooling. The final library pool was sequenced on the Illumina Hiseq instrument using 150-base-pair paired-end reads. Briefly, 6-10 billion base calls were generated for each sample. PCR was performed with the same PCR primer cocktail used in TruSeq DNA Sample Preparation. The pipeline of raw data processing and calling was as follows. Quality control of raw data was conducted with Fast QC software (http://www.bioinformatics.babraham.ac.uk/projects/fastqc/). Reads were mapped to reference the genome build using the Burrows-Wheeler Alignment tool (BWA). The duplicate reads were flagged using Picard-tools (http://picard.sourceforge.net/). Gene expression levels

were quantified as transcripts per million (TPM), which were calculated as the number of UMIs of each gene divided by all the UMIs of a given cell and multiplied by 1,000,000. Three key parameters (number of RNA features greater than 200 and less than 7500, percentage of mitochondria less than 10, and percentage of read cells less than 10) were used for filtering the raw cells. The parameter of resolution in cluster finding was determined as 0.6.

Data processing tools

All data processing was based on R platform (version 3.6.2, https://www.R-project.org/). Seurat (http://satijalab.org/seurat/install.html) was employed for cell clustering. Pseudotime trajectory analysis was performed with Monocle (http://bioconductor.org/packages/release/bioc/html/monocle.html). Pheatmap (https://cran.r-project.org/web/packages/pheatmap/index.html) was used for plotting the heatmap. Pathway descriptions (GO and KEGG enrichment analysis) were demonstrated by clusterProfiler (http://bioconductor.org/packages/release/bioc /html/clusterProfiler.html). The p values were calculated using Pearson's correlation. Values of $p < 0.05$ were considered significant.

Immunohistochemistry and immunofluorescence staining

All antibodies applied in current assays are listed in Table S6. Briefly, bladder tissue frozen sections were placed directly on the slide, and then fixed with an immunostaining fixative (Beyotime, #P0098, China). Then, the slides were washed twice with immunostaining washing solution (Beyotime, #P0106, China) for 5 minutes each. The immunostaining blocking solution (Beyotime, #P0102, China) was added and blocked overnight at 4°C. The primary antibody was diluted to the appropriate ratio according to the instructions with the QuickBlock™ Primary antibody dilution buffer (Beyotime, #P0262, China), and then added to the sections and incubated overnight at 4°C with slow shaking. Immunostaining washing solution was then added and washed slowly by shaking on a side shaker for 5 minutes; this was repeated 3 times. Based on the instruction manual of the secondary antibody, dilution with the immunofluorescent secondary antibody buffer (Beyotime, #P0106, China) or with immunohistochemistry secondary antibody solution (Beyotime, #P0110, China) was performed. Immunostaining washing solution was added and washed slowly by shaking on a side shaker for 5 minutes, repeated 3 times. The results were observed using the appropriate tools.

Flow cytometric sorting and transmission electron microscopy (TEM)

The cell surface staining procedure of human cell suspensions was performed as per the instructions of BD Biosciences. Briefly, cells were resuspended in BD Pharmingen Stain Buffer (BSA) (Cat. No. 554657), then added with 1 ml of precooled BSA, and centrifuged at 4°C for 5 minutes. This was repeated 2 times. The final cell concentration was adjusted to 2×10^7 cells/ml with BSA and 100 µl of the cell suspension

(106 cells) was transferred to a 12 x 75 mm round bottom polypropylene test tube. Then, 5 μl of the surface antibody (CD90) was added to each tube and incubated for 20 minutes on ice, in the dark. The cells were washed twice with an appropriate amount of Stain Buffer, and centrifuged at 300 x *g* for 5 minutes. The tube or microplate was tapped to mix the cells, and flow cytometry was performed to filter $CD90^+$ cells.

Cells in a 10 cm dish were collected and fixed with 2.5% glutaraldehyde in phosphate buffer solution for 2 hours, rinsed with 0.1M phosphoric acid for 15 minutes, 3 times.

Subsequently, 1% acetic acid fixative was added for 2-3 hours and rinsed with 0.1 M phosphoric acid for 15 minutes, 3 times. Dehydration treatment was performed at 4°C with 50% ethanol for 15 minutes, 70% ethanol for 15 minutes, 90% ethanol for 15 minutes, 90% ethanol and 90% acetone for 15 minutes, and 90% acetone for 20 minutes, separately. Cells were embedded in pure embedding solutions at 37°C for 3 hours, and cured in a 45°C oven for 12 hours. After ultra-thin microtome slicing at 50 nm, sections were stained with 3% uranium acetate-lead citrate. The stained sections were observed by TEM and the results were recorded.

Abbreviations

t-SNE, t-Distributed stochastic neighbor embedding

TEM , Transmission electron microscope

KEGG, Kyoto Encyclopedia of Genes and Genomes

Declarations

Ethics approval and consent to participate

The current investigation was conducted with the approval of the medical ethics committee of the Second Affiliated Hospital of the Army Medical University. Each patient signed a written informed consent form before donating their tissues for this study.

Consent for publication

All authors read and approved the final manuscript.

Availability of data and material

The datasets used or analyzed during the current study are available from the corresponding author on reasonable request.

Competing interests

The authors declare no competing interests.

Funding

The project was supported partly by grants from National Natural Science Foundation of China (8160058 and 81873628), and partly by grants from Major Program of National Natural Science Foundation of China (81930017). Special thanks give for Genergy Technology Co.,Ltd., Shanghai to do 10x genomic sequencing for us.

Authors' contributions

Z.Y. and L.L. conceived the project, and J.Z. and Y.Z. were involved in designing the study. W.J., Z.F. and J.Z. were responsible for the tissue sample collection. Z.Y., Y.G. and P.L. performed the experiments. Z.Y. and J.Z. conducted the bioinformatics analysis. Z.Y. and L.L. supervised the project, wrote the manuscript, and responsible for all data present in current research.

Acknowledgements

Not applicable.

References

1. Andersson K-E, Arner A: **Urinary bladder contraction and relaxation: physiology and pathophysiology**. *Physiological reviews* 2004, **84**(3):935-986.
2. Birder L, Andersson K-E: **Urothelial signaling**. *Physiological reviews* 2013, **93**(2):653-680.
3. Fry CH: **Interstitial cells in the urinary tract, where are they and what do they do?** *BJU international* 2014, **114**(3):434-435.
4. Drumm BT, Koh SD, Andersson KE, Ward SM: **Calcium signalling in Cajal-like interstitial cells of the lower urinary tract**. *Nature reviews Urology* 2014, **11**(10):555-564.
5. Monaghan KP, Johnston L, McCloskey KD: **Identification of PDGFRalpha positive populations of interstitial cells in human and guinea pig bladders**. *The Journal of urology* 2012, **188**(2):639-647.
6. Johnston L, Woolsey S, Cunningham RM, O'Kane H, Duggan B, Keane P, McCloskey KD: **Morphological expression of KIT positive interstitial cells of Cajal in human bladder**. *The Journal of urology* 2010, **184**(1):370-377.
7. Gevaert T, Vanstreels E, Daelemans D, Franken J, Van Der Aa F, Roskams T, De Ridder D: **Identification of different phenotypes of interstitial cells in the upper and deep lamina propria of the human**

bladder dome. *The Journal of urology* 2014, **192**(5):1555-1563.

8. Drake MJ, Fry CH, Eyden B: **Structural characterization of myofibroblasts in the bladder**. *BJU international* 2006, **97**(1):29-32.
9. Vannucchi MG, Traini C, Guasti D, Del Popolo G, Faussone-Pellegrini MS: **Telocytes subtypes in human urinary bladder**. *Journal of cellular and molecular medicine* 2014, **18**(10):2000-2008.
10. Gandhi D, Molotkov A, Batourina E, Schneider K, Dan H, Reiley M, Laufer E, Metzger D, Liang F, Liao Y: **Retinoid signaling in progenitors controls specification and regeneration of the urothelium**. *Developmental cell* 2013, **26**(5):469-482.
11. McCloskey KD: **Bladder interstitial cells: an updated review of current knowledge**. *Acta physiologica (Oxford, England)* 2013, **207**(1):7-15.
12. Lang RJ, Klemm MF: **Interstitial cell of Cajal-like cells in the upper urinary tract**. *Journal of cellular and molecular medicine* 2005, **9**(3):543-556.
13. Davidson RA, McCloskey KD: **Morphology and localization of interstitial cells in the guinea pig bladder: structural relationships with smooth muscle and neurons**. *The Journal of urology* 2005, **173**(4):1385-1390.
14. Buoro S, Ferrarese P, Chiavegato A, Roelofs M, Scatena M, Pauletto P, Passerini-Glazel G, Pagano F, Sartore S: **Myofibroblast-derived smooth muscle cells during remodelling of rabbit urinary bladder wall induced by partial outflow obstruction**. *Laboratory investigation; a journal of technical methods and pathology* 1993, **69**(5):589-602.
15. Fry C, Sui GP, Kanai A, Wu C: **The function of suburothelial myofibroblasts in the bladder**. *Neurourology and Urodynamics: Official Journal of the International Continence Society* 2007, **26**(S6):914-919.
16. Grol S, Essers PB, van Koeveringe GA, Martinez-Martinez P, de Vente J, Gillespie JI: **M(3) muscarinic receptor expression on suburothelial interstitial cells**. *BJU international* 2009, **104**(3):398-405.
17. Kuijpers KA, Heesakkers JP, Jansen CF, Schalken JA: **Cadherin-11 is expressed in detrusor smooth muscle cells and myofibroblasts of normal human bladder**. *European urology* 2007, **52**(4):1213-1221.
18. Drake MJ, Hedlund P, Andersson KE, Brading AF, Hussain I, Fowler C, Landon DN: **Morphology, phenotype and ultrastructure of fibroblastic cells from normal and neuropathic human detrusor: absence of myofibroblast characteristics**. *The Journal of urology* 2003, **169**(4):1573-1576.
19. Neuhaus J, Schroppel B, Dass M, Zimmermann H, Wolburg H, Fallier-Becker P, Gevaert T, Burkhardt CJ, Do HM, Stolzenburg JU: **3D-electron microscopic characterization of interstitial cells in the human bladder upper lamina propria**. *Neurourology and urodynamics* 2018, **37**(1):89-98.
20. Sun X, Kaufman PD: **Ki-67: more than a proliferation marker**. *Chromosoma* 2018, **127**(2):175-186.
21. Kloskowski T, Uzarska M, Gurtowska N, Olkowska J, Joachimiak R, Bajek A, Gagat M, Grzanka A, Bodnar M, Marszałek A: **How to isolate urothelial cells? Comparison of four different methods and literature review**. *Human cell* 2014, **27**(2):85-93.

22. Pokrywczynska M, Balcerczyk D, Jundzill A, Gagat M, Czapiewska M, Kloskowski T, Nowacki M, Gastecka AM, Bodnar M, Grzanka A: **Isolation, expansion and characterization of porcine urinary bladder smooth muscle cells for tissue engineering**. *Biological procedures online* 2016, **18**(1):17.
23. Aitken KJ, Bägli DJ: **The bladder extracellular matrix. Part I: architecture, development and disease**. *Nature Reviews Urology* 2009, **6**(11):596.
24. Lee H, Koh BH, Peri LE, Sanders KM, Koh SD: **Functional expression of SK channels in murine detrusor PDGFRα+ cells**. *The Journal of physiology* 2013, **591**(2):503-513.

Figures

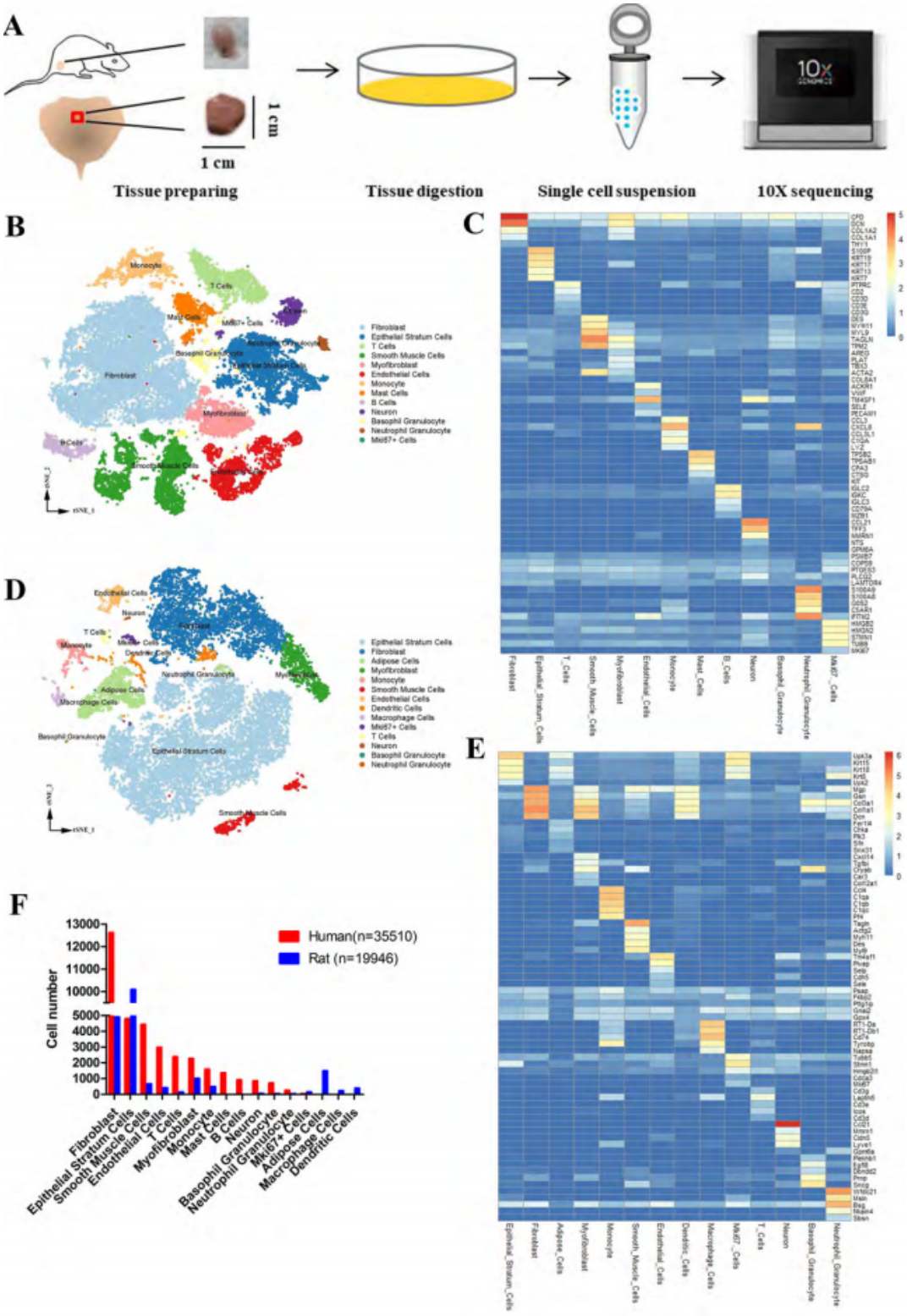

Figure 1

10x Single-cell RNA-seq analysis of human and rat bladder. a A schematic representation of experiment processing. b t-Distributed stochastic neighbor embedding (t-SNE) analysis of all of the filtered cells (n=35510) from human bladder tissues. c Heatmap showing scaled expression levels for marker genes of each cluster in human bladder. d t-SNE analysis of all of the filtered cells (n=19946) from rat bladder. e

Heatmap showing scaled expression levels for marker genes of each cluster in rat bladder. f Comparison of cell numbers of each cluster in human and rat bladder.

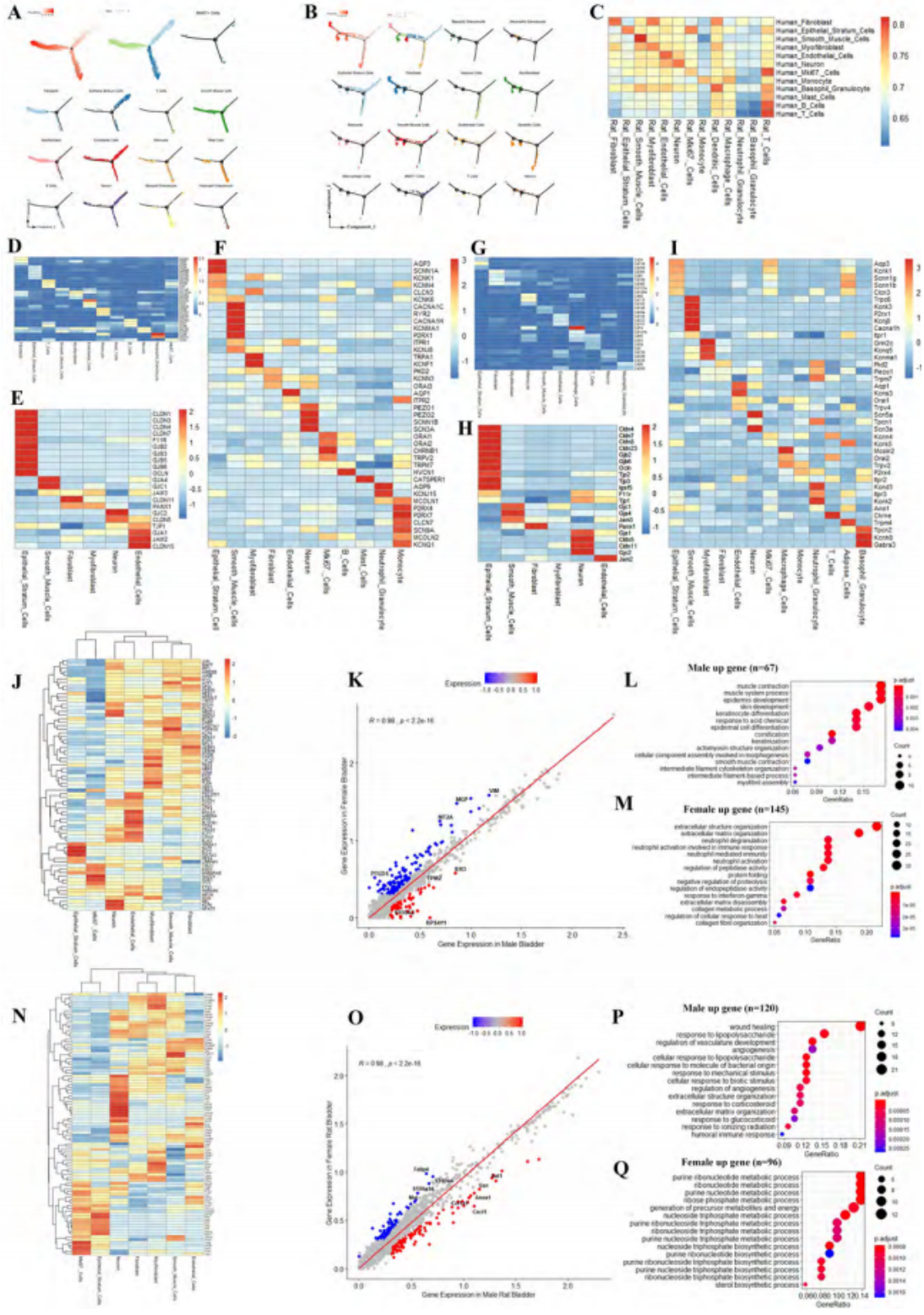

Figure 2

Characterize of each cell types in human and rat Bladder. a Pseudotime trajectory analysis showing the distribution of 13 cell types in human bladder. b Pseudotime trajectory analysis showing the distribution of 14 cell types in rat bladder. c Heatmap showing Pearson correlation of average expression level

between cell types from human (horizontal) and rat (vertical) bladder tissue. d Heatmap showing scaled expression levels for marker CD molecular of 12 cell types in human bladder. e Heatmap showing scaled expression levels for junction genes of 6 cell types in human bladder. f Heatmap showing scaled expression levels for receptor and ion channel of 11 cell types in human bladder. g Heatmap showing scaled expression levels for marker Cd molecular of 10 cell types in rat bladder. h Heatmap showing scaled expression levels for junction genes of 6 cell types in rat bladder. i Heatmap showing scaled expression levels for receptor and ion channel of 6 cell types in rat bladder. j Heatmap showing scaled expression levels for transcription factors of 7 cell types in human bladder. k Scatterplot shows average expression level of all genes (n=27709) between human male (horizontal) and female (vertical) bladder tissue. l GO enrichment analysis of high expression genes (n=67) in human male bladder tissue. m GO enrichment analysis of high expression genes (n=145) in human female bladder tissue. n Heatmap showing scaled expression levels for transcription factors of 7 cell types in rat bladder. o Scatterplot shows average expression level of all genes (n=25199) between rat male (horizontal) and female (vertical) bladder tissue. p GO enrichment analysis of high expression genes (n=120) in rat male bladder tissue. q GO enrichment analysis of high expression genes (n=96) in rat female bladder tissue.

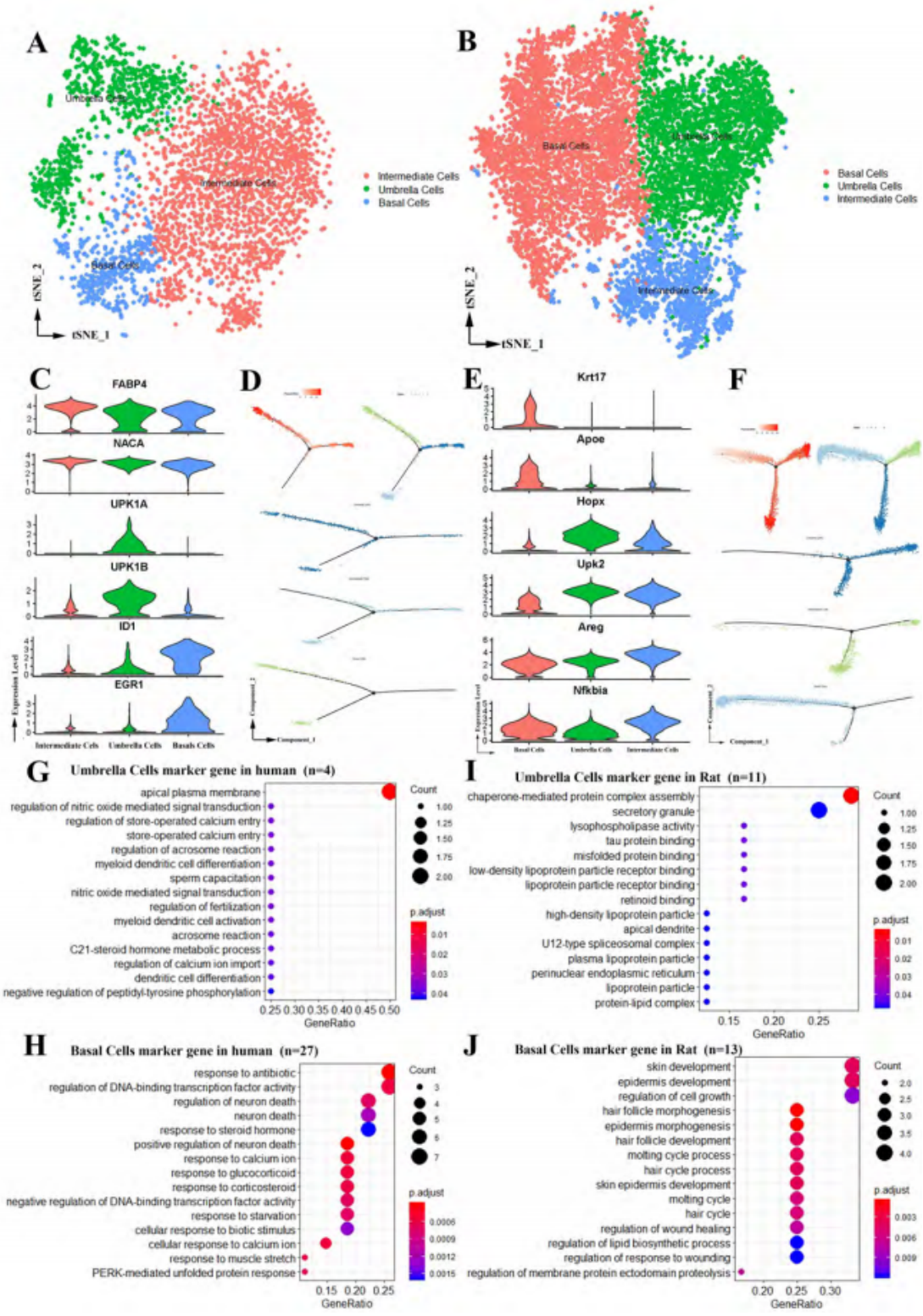

Figure 3

Characterize of epithelial stratum cells. a t-SNE analysis of epithelial stratum cells (n=4784) from human bladder. b t-SNE analysis of epithelial stratum cells (n=10081) from rat bladder. c Violin plots indicating average expression level of marker genes for 3 clusters of epithelial stratum cells in human bladder. d Pseudotime trajectory analysis showing the distribution of 3 clusters of epithelial stratum cells in human bladder. e Violin plots indicating average expression level of marker genes for 3 clusters of epithelial

stratum cells in rat bladder. f Pseudotime trajectory analysis showing the distribution of 3 clusters of epithelial stratum cells in rat bladder. g GO enrichment analysis of marker genes (n=4) in umbrella cells of human. h GO enrichment analysis of marker genes (n=27) in basal cells of human. i GO enrichment analysis of marker genes (n=11) in umbrella cells of rat. j GO enrichment analysis of marker genes (n=13) in basal cells of rat.

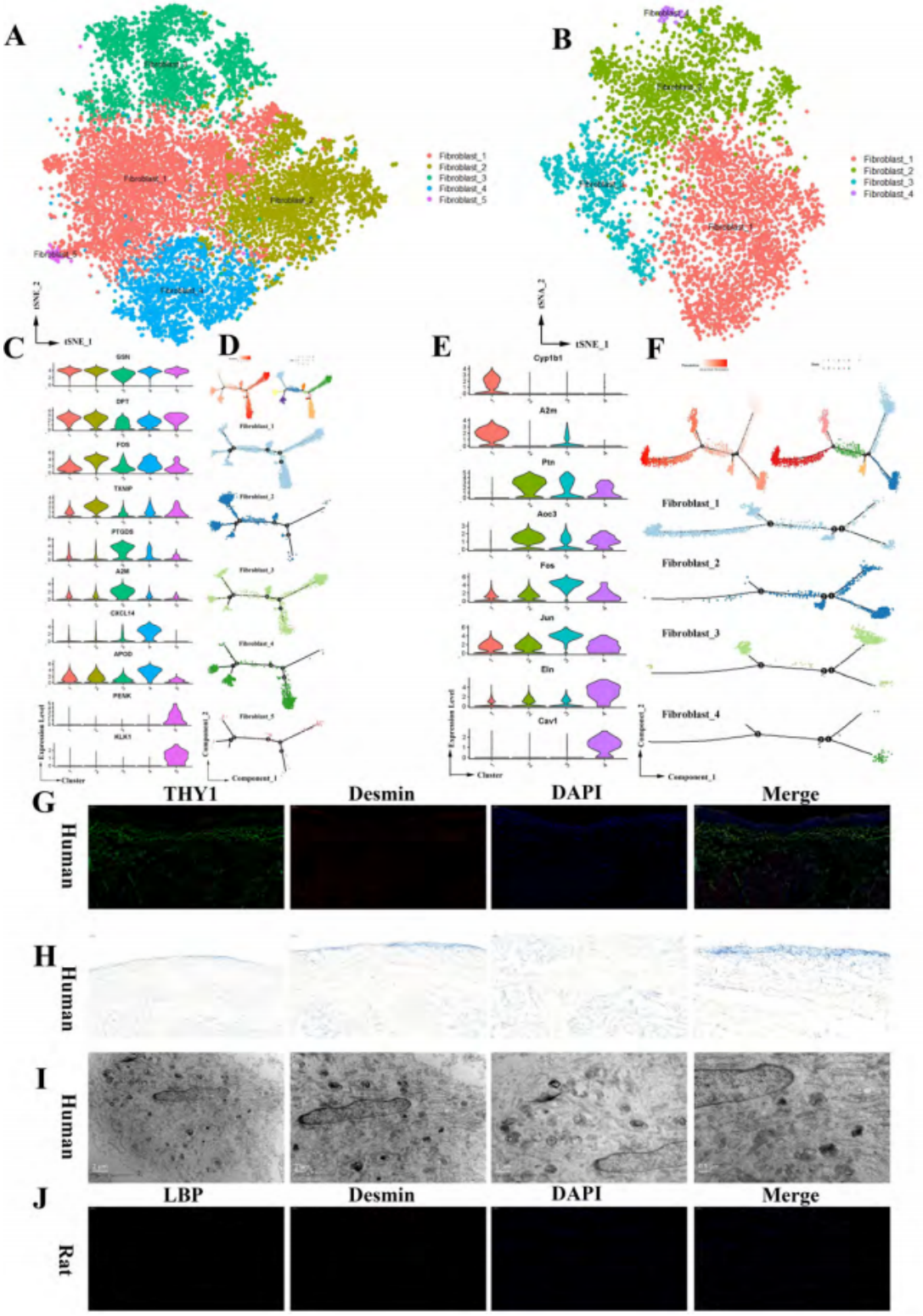

Figure 4

Characterize of fibroblast-like cells. a t-SNE analysis of fibroblast cells (n=12615) from human bladder. b t-SNE analysis of fibroblast cells (n=4898) from rat bladder. c Violin plots indicating average expression level of marker genes for 5 clusters of fibroblast cells in human bladder. d Pseudotime trajectory analysis showing the distribution of 5 clusters of fibroblast cells in human bladder. e Violin plots indicating average expression level of marker genes for 4 clusters of fibroblast cells in rat bladder. f Pseudotime trajectory analysis showing the distribution of 4 clusters of fibroblast cells in rat bladder. g Double immunofluorescence staining performed with anti-THY1 and anti-DES antibody using human bladder tissues. h Immunohistochemistry staining performed with anti-THY1 antibody using human bladder tissues. i Transmission electron microscope (TEM) scanning of CD90+ fibroblast cells from human bladder tissues. j Double immunofluorescence staining performed with anti-LBP and anti-Des antibody using rat bladder tissues.

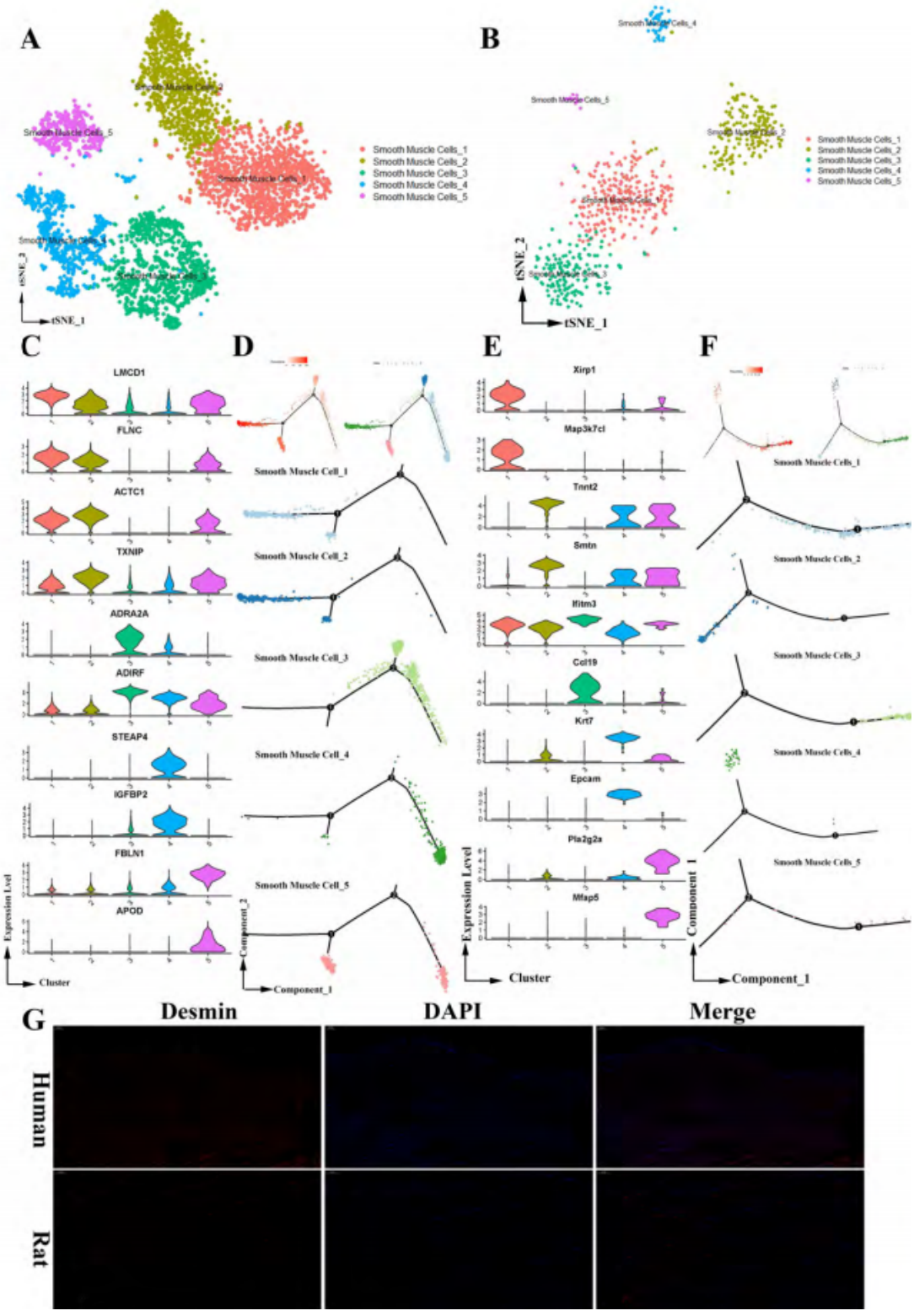

Figure 5

Characterize of smooth muscle cells. a t-SNE analysis of smooth muscle cells (n=4429) from human bladder. b t-SNE analysis of smooth muscle cells (n=644) from rat bladder. c Violin plots indicating average expression level of marker genes for 5 clusters of smooth muscle cells in human bladder. d Pseudotime trajectory analysis showing the distribution of 5 clusters of smooth muscle cells in human bladder. e Violin plots indicating average expression level of marker genes for 5 clusters of smooth

muscle cells in rat bladder. f Pseudotime trajectory analysis showing the distribution of 5 clusters of smooth muscle cells in rat bladder. g Immunofluorescence staining performed with anti-Des antibody in human and rat bladder.

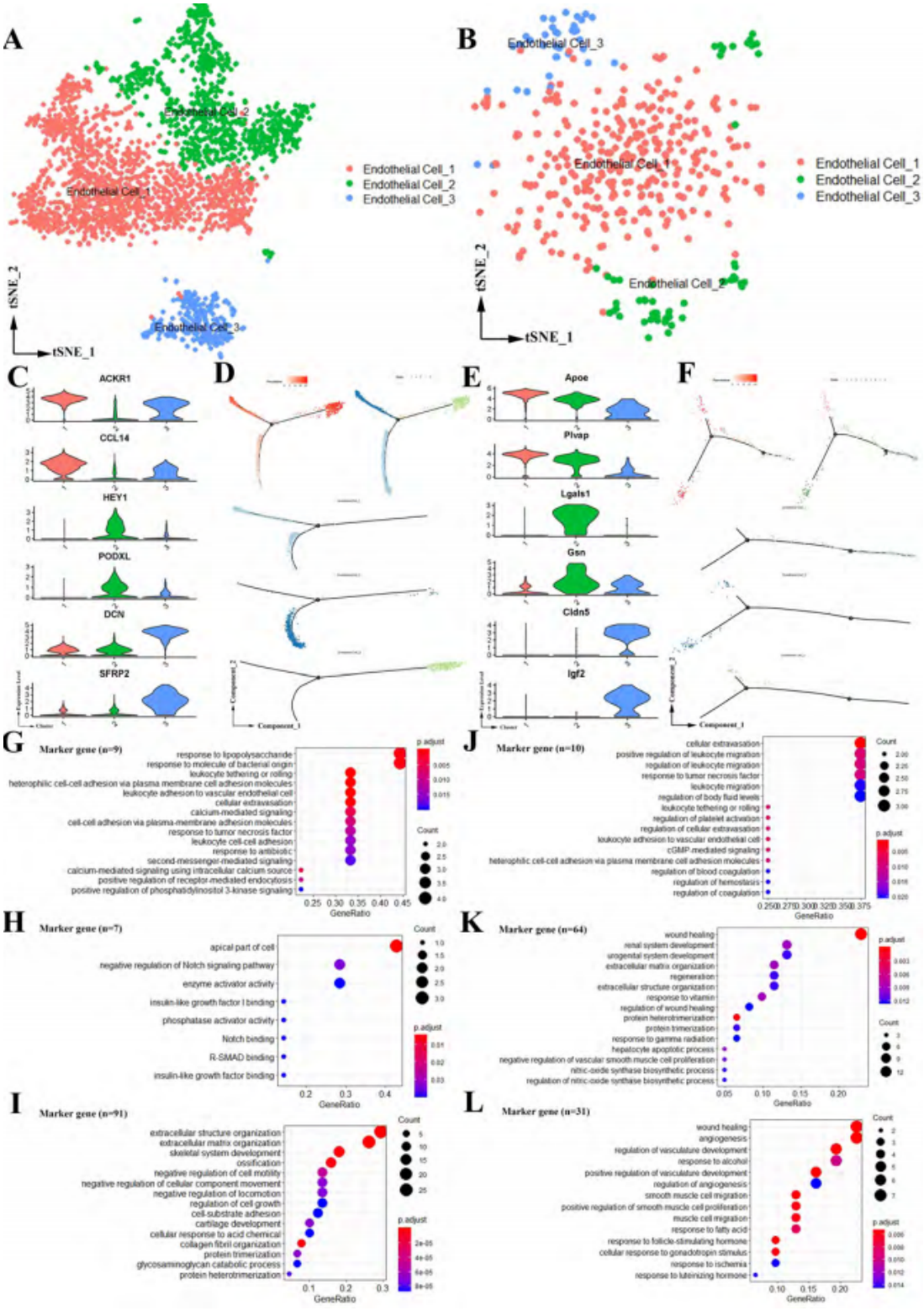

Figure 6

Characterize of endothelial cells. a t-SNE analysis of endothelial cells (n=2971) from human bladder. b t-SNE analysis of endothelial cells (n=405) from rat bladder. c Violin plots indicating average expression

level of marker genes for 3 clusters of endothelial cells in human bladder. d Pseudotime trajectory analysis showing the distribution of 3 clusters of endothelial cells in human bladder. e Violin plots indicating average expression level of marker genes for 3 clusters of endothelial cells in rat bladder. f Pseudotime trajectory analysis showing the distribution of 3 clusters of endothelial cells in rat bladder. g GO enrichment analysis of marker genes (n=9) in endothelial cell_1 of human bladder. h GO enrichment analysis of marker genes (n=7) in endothelial cell_2 of human bladder. i GO enrichment analysis of marker genes (n=91) in endothelial cell_3 of human bladder. j GO enrichment analysis of marker genes (n=10) in endothelial cell_1 of rat bladder. k GO enrichment analysis of marker genes (n=64) in endothelial cell_2 of rat bladder. l GO enrichment analysis of marker genes (n=31) in endothelial cell_3 of rat bladder.

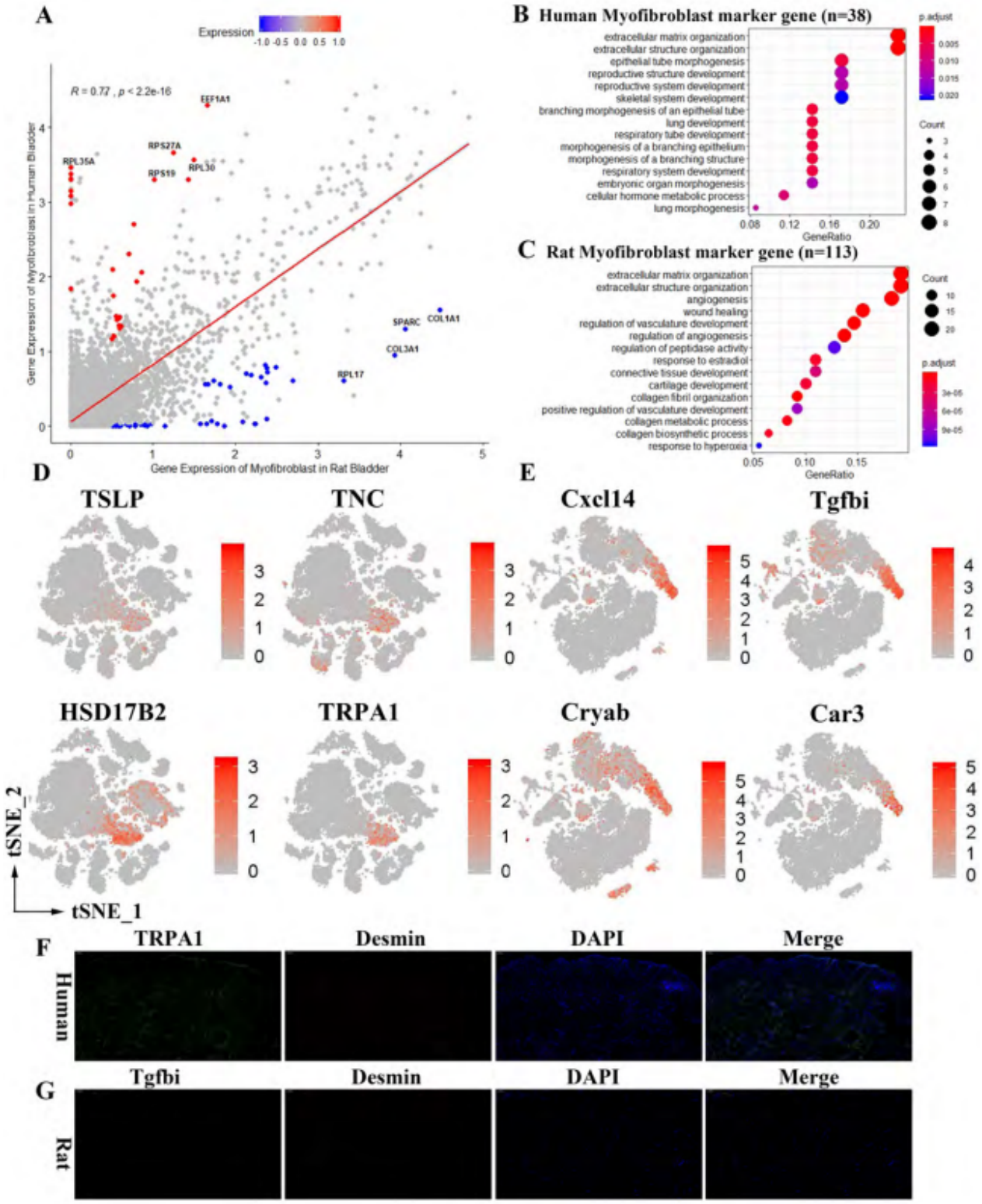

Figure 7

Characterize of myofibroblast cells. a Scatterplot shows average expression level of homologous genes (n=15106) between rat (horizontal) and human (vertical) myofibroblast cells. b GO enrichment analysis of high expression level genes (n=38) in myofibroblast cells of human bladder. c GO enrichment analysis of high expression level genes (n=113) in myofibroblast cells of rat bladder. d Feature plots of 4 characteristic marker genes in all human bladder cells and their expression level (shown as gradient of

red). e Feature plots of 4 characteristic marker genes in all rat bladder cells and their expression level (shown as gradient of red). f Double immunofluorescence staining performed with anti-TRPA1 and anti-DES antibody using human bladder. g Double immunofluorescence staining performed with anti-Tgfbi and anti-Des antibody using rat bladder.

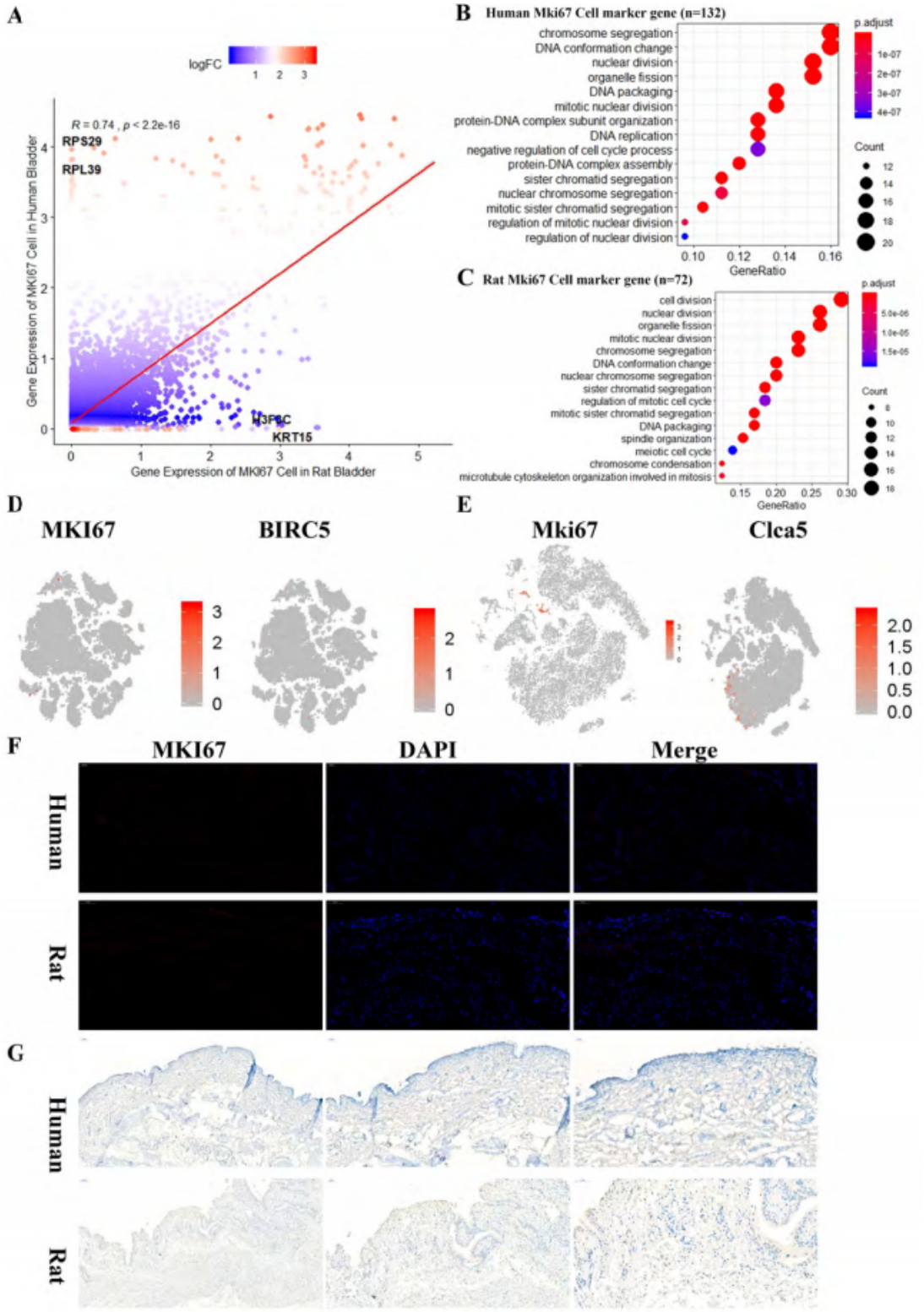

Figure 8

Characterize of Mki67+ cells. a Scatterplot shows average expression level of homologous genes (n=15106) between rat (horizontal) and human (vertical) Mki67+ cells. b GO enrichment analysis of high expression level genes (n=132) in Mki67+ cells of human bladder. c GO enrichment analysis of high expression level genes (n=72) in Mki67+ cells of rat bladder. d Feature plots of 2 characteristic marker genes in all human bladder cells and their expression level (shown as gradient of red). e Feature plots of 2 characteristic marker genes in all rat bladder cells and their expression level (shown as gradient of red). f Immunofluorescence staining performed with anti-MKI67 antibody using human and rat bladder. g Immunohistochemistry staining performed with anti-MKI67 antibody using human and rat bladder.

Supplementary Files

This is a list of supplementary files associated with this preprint. Click to download.

- ARRIVEguidelines.docx
- Supplementarytables.xlsx
- SupplementaryFigures.pdf